Two polymorphic Co(II) field-induced single-ion magnets with enormous angular distortion from the ideal octahedron

I. Nemec, R. Herchel and Z. Trávníček*

Regional Centre of Advanced Technologies and Materials, Department of Inorganic Chemistry, Faculty of Science, Palacký University, 17. listopadu 12, CZ-771 46 Olomouc, Czech Republic.

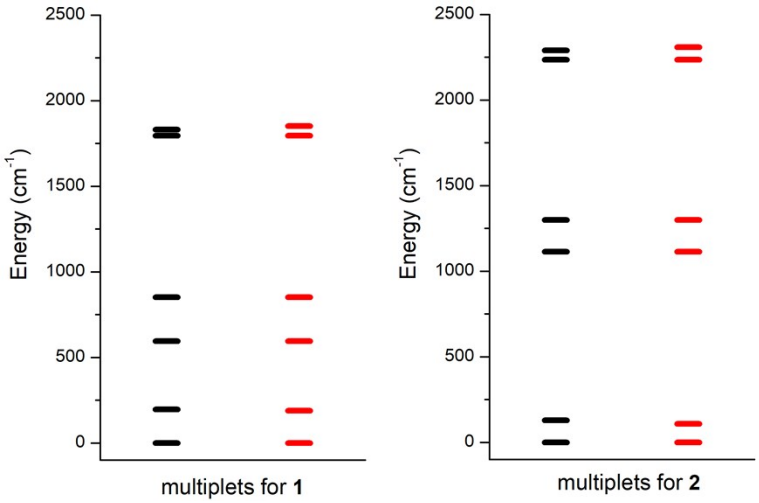

Figure S1 The multiplet energy levels calculated by CASSCF/NEVPT2 (black) and reconstructed energy levels with Figgis-Griffith Hamiltonian (eq.1) (red) with $\alpha\cdot\lambda$ = -236 cm^{-1}, Δ_{ax} = -1269 cm^{-1}, Δ_{rh} = -181 cm^{-1} for **1** and with $\alpha\cdot\lambda$ = -246 cm^{-1}, Δ_{ax} = +1522 cm^{-1}, Δ_{rh} = +489 cm^{-1} for **2**.

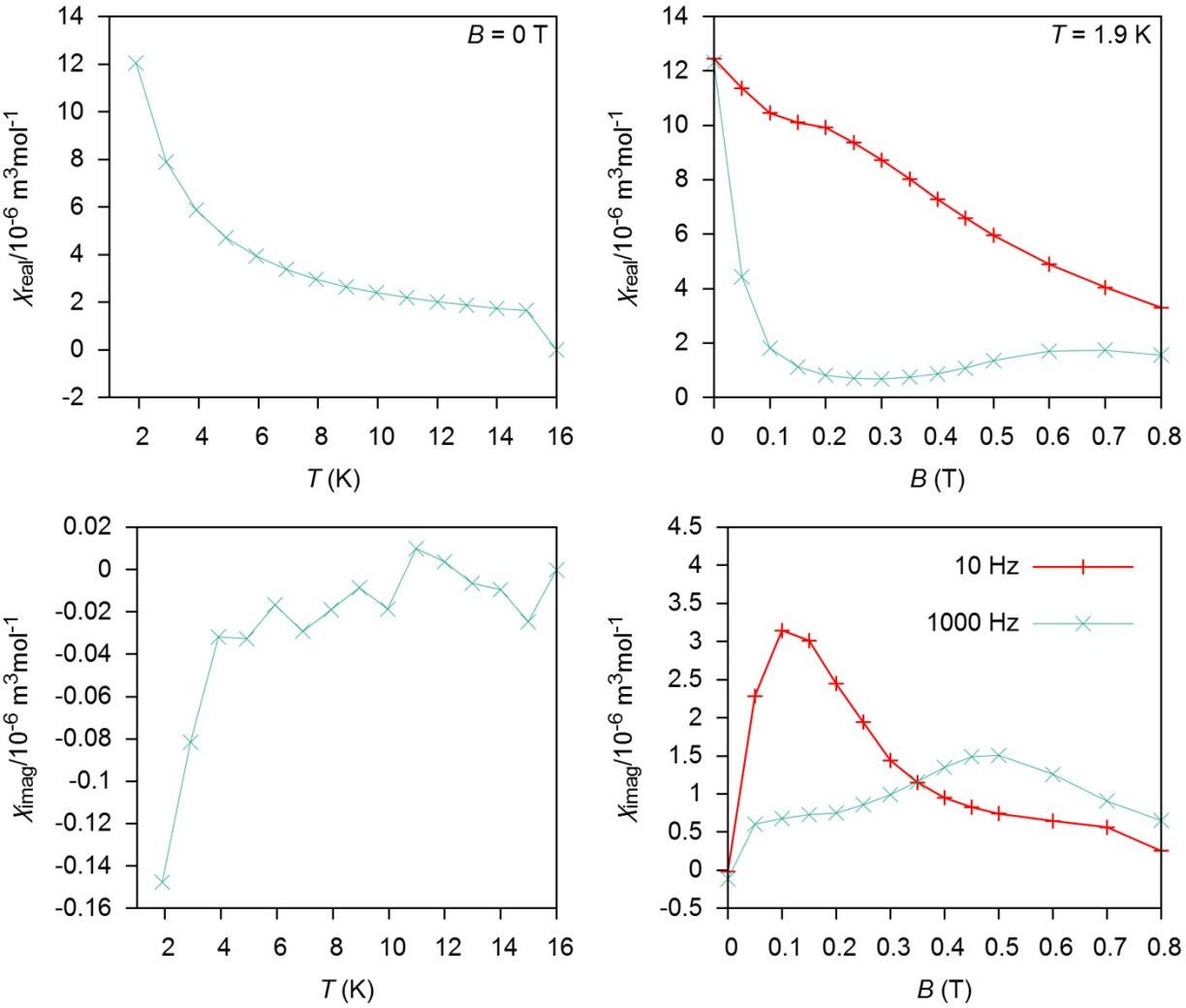

Figure S2 In-phase χ_{real} and out-of-phase χ_{imag} molar susceptibilities for **1** at zero static magnetic field (*left*) and in non-zero static field (*right*). Lines serve as guides for the eyes.

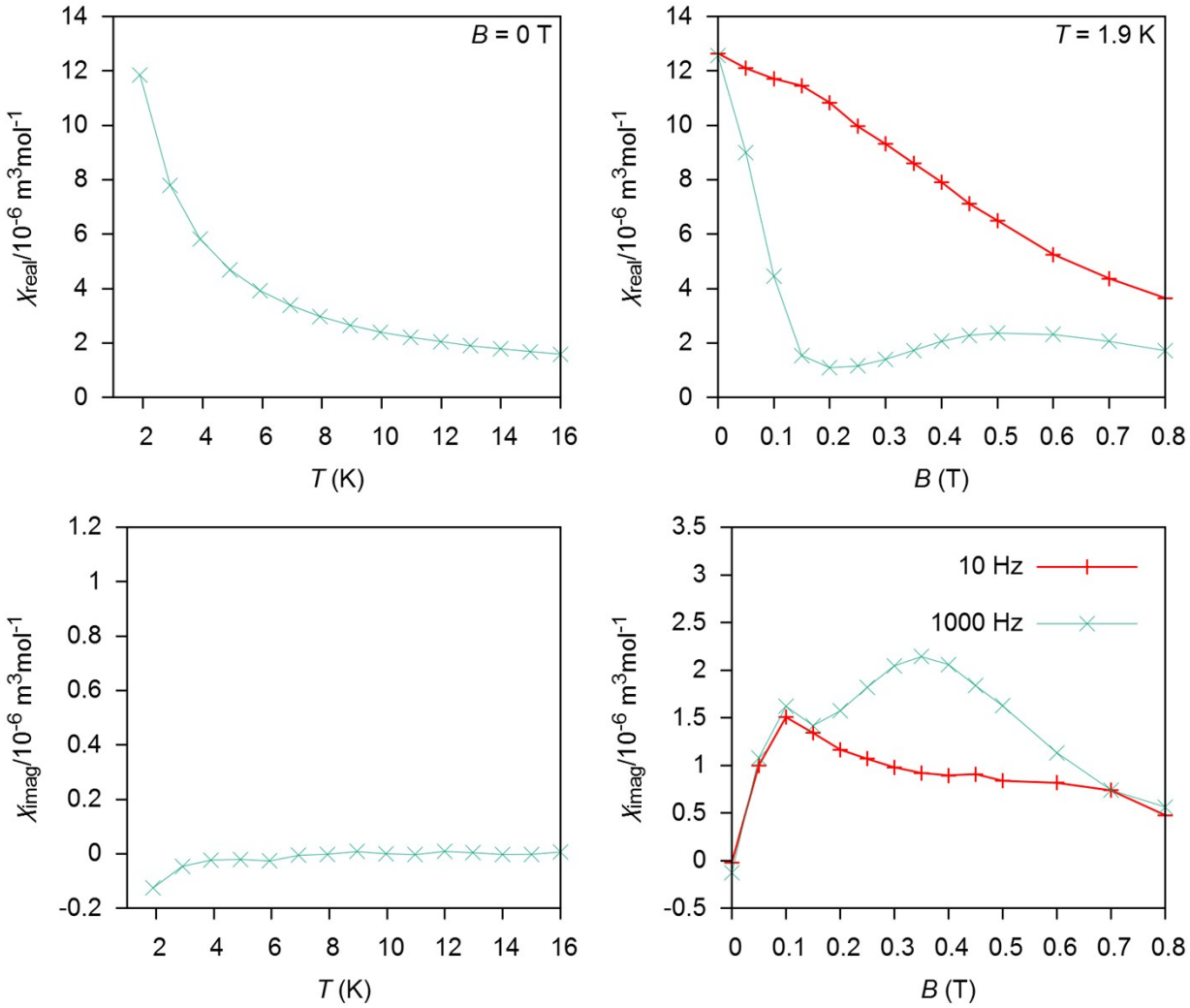

Figure S3 In-phase χ_{real} and out-of-phase χ_{imag} molar susceptibilities for **2** at zero static magnetic field (*left*) and in non-zero static field (*right*). Lines serve as guides for the eyes.

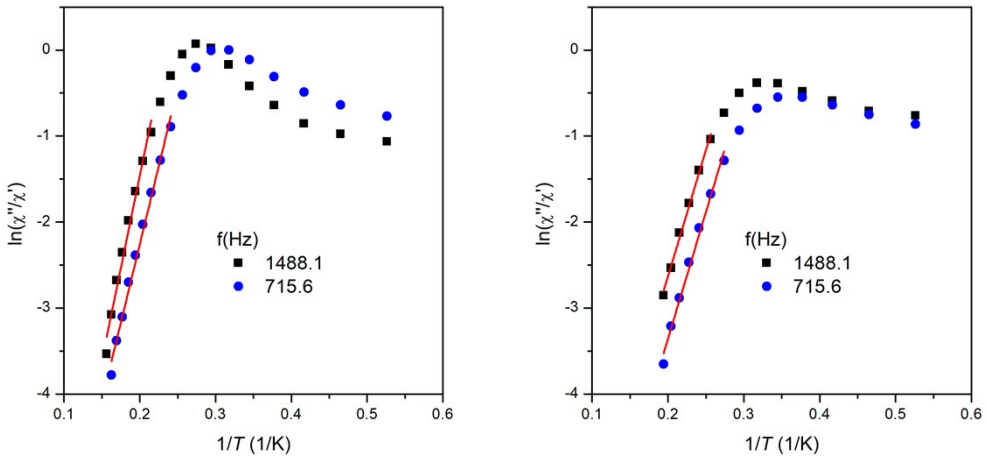

Figure S4 Analysis of in-phase χ' and out-of-phase χ'' molar susceptibilities for **1** (left) and **2** (right) measured at the applied external field B_{dc} = 0.1 T according to eq. 8. Full points – experimental data, full lines – calculated data.

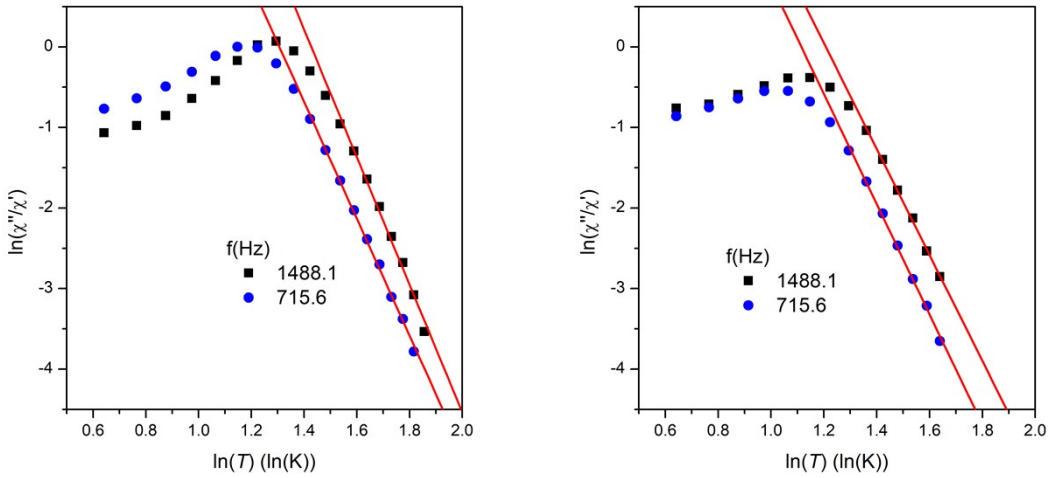

Figure S5 Analysis of in-phase χ' and out-of-phase χ'' molar susceptibilities for **1** (left) and **2** (right) measured at the applied external field B_{dc} = 0.1 T according to eq. 10. Full points – experimental data, full lines – calculated data.

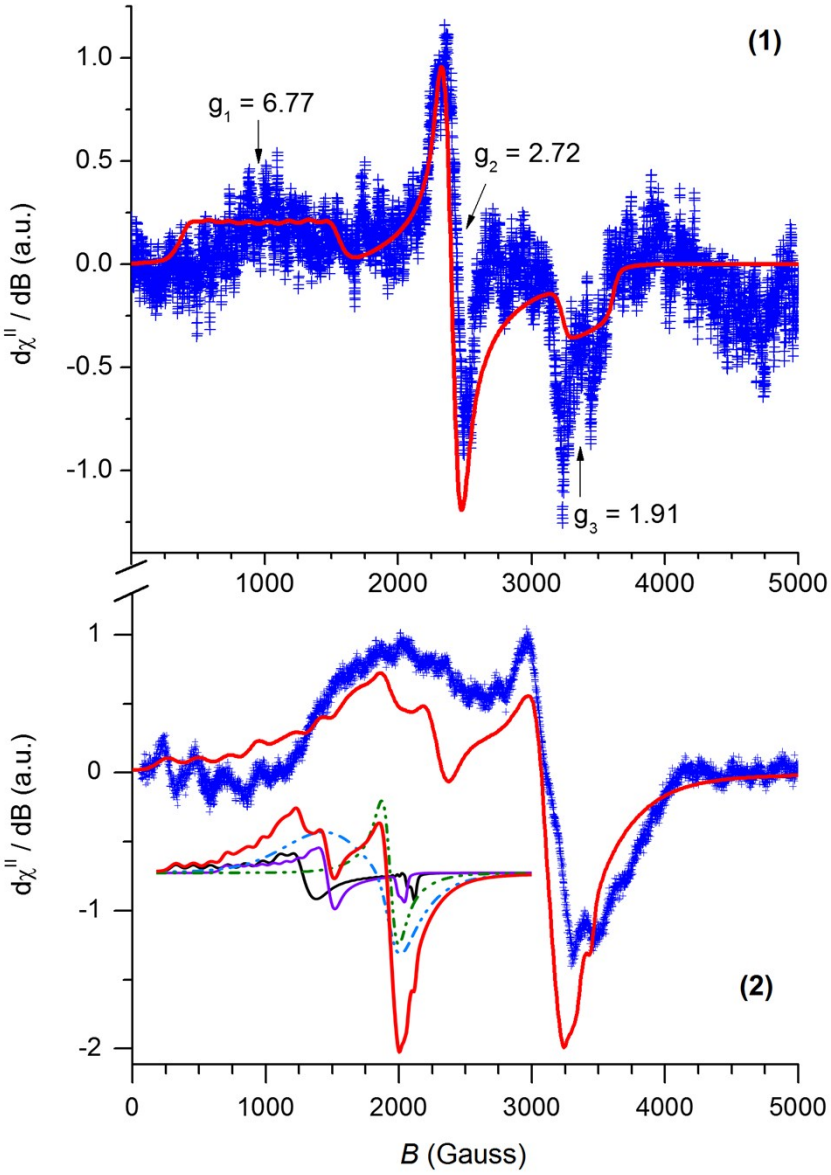

Figure S6 Low temperature (*T* = 113 K) X-band EPR spectra of compounds (**1**, upper) and (**2**, lower)**.** Simulation of the EPR resonances are shown by red-lines. Experimental parameters for (**1**): 9.141 GHz Frequency, 100 KHz modulation frequency, 100 ms time constant, 0.8 mT modulation width, 2.00 mW of applied microwave power, 8 min sweep-time, 10 scans accumulated and averaged. Experimental parameters for (**2**) 9.169 GHz Frequency, 100 KHz modulation frequency, 100 ms time constant, 0.8 mT modulation width, 2.60 mW of applied microwave power, 8 min sweep-time, 20 scans accumulated and averaged.

Table S1. Crystal data and structure refinement parameters for compounds **2** and **3**.

Formula	$C_{28}H_{21}CoN_2O_4$	$C_{28}H_{21}N_2O_4Zn$
M (g·mol^{-1})	508.42	511.86
Crystal system	Monoclinic	Monoclinic
Space group	$P2_1/n$	$C2/c$
λ (Å)	0.71073	0.71073
a (Å)	11.2960(6)	17.722(3)
b (Å)	15.9061(9)	14.424(3)
c (Å)	13.4636(8)	9.2768(13)
β (°)	106.951(6)	91.848(6)
V (Å^3)	2314.0(2)	2370.1(7)
Z	4	4
T (K)	150(2)	150(2)
ρ_{calcd} (g·cm^{-3})	1.459	1.434
μ (mm^{-1})	0.780	1.070
Data/restraints/ parameters	4061/0/318	2953/0/160
$R_1{}^a$ [I > 2σ(I)]/R_1 (all)	0.0395/0.0573	0.0392/0.0600
$wR_2{}^b$ [I > 2σ(I)]/wR_2 (all)	0.0874/0.0915	0.1121/0.1302
Goodness-of-fit	1.032	0.964
largest peak and hole (e Å^{-3})	0.579 and -0.261	0.503/-0.427
CCDC number	1581344	1581345

Table S2 The results of the SHAPE calculations for molecular structures of **1** and **2**.

compound	**HP-6**	**PPY-6**	**OC-6**	**TPR-G**	**JPPY-6**
1	26.920	19.371	6.826	12.250	22.704
2	28.242	19.857	6.432	10.685	22.680

HP-6 (D6h), Hexagon; PPY-6, (C_{5v}), Pentagonal pyramid; OC-6, (O_h), Octahedron, TPR-6, (D_{3h}), Trigonal prism; JPPY-6, (C_{5v}); Johnson pentagonal pyramid, J2.

Table S3. Parameters of one-component Debey model for **1** derived according eq. 4 in the main text.

T/K	$\chi_S/(10^{-6}\ m^3\ mol^{-1})$	$\chi_T/(10^{-6}\ m^3\ mol^{-1})$	α	$\tau/(10^{-4}\ s)$
1.90	1.57	12.37	0.167	54.0
2.15	1.37	10.87	0.143	37.9
2.40	1.27	9.83	0.139	27.9
2.65	1.16	8.90	0.099	18.1
2.90	1.08	8.16	0.089	11.6
3.15	1.05	7.48	0.050	7.1
3.40	1.02	6.95	0.032	4.4
3.65	0.94	6.51	0.032	2.7

Table S4. Parameters of one-component Debey model for **2** derived according eq. 4 in the main text.

T/K	$\chi_S/(10^{-6}\ m^3\ mol^{-1})$	$\chi_T/(10^{-6}\ m^3\ mol^{-1})$	α	$\tau/(10^{-4}\ s)$
1.90	2.91	12.61	0.266	19.7
2.15	2.54	11.12	0.236	11.8
2.40	2.40	10.05	0.190	8.3
2.65	2.27	9.04	0.152	5.3
2.90	2.18	8.26	0.108	3.3
3.15	1.44	7.62	0.097	1.9